An Antiproton Target Design for Increased Beam Intensity

K. Anderson, C.M. Bhat, J. Marriner, and Z. Tang
Fermi National Accelerator Laboratory *
P.O. Box 500
Batavia, Illinois 60510

Abstract

Upon the commissioning of the higher energy LINAC and Main Injector at FNAL, increased proton beam intensities will be achieved. Despite these upgrades, the target used in the production of antiprotons must maintain mechanical integrity when exposed to the more intense primary proton beam. This paper describes the design parameters and thermal bench testing of an efficient air cooled target designed for effective bulk cooling and dynamic stress wave amplitude control when the target is exposed to a 120 GeV primary proton beam of 1.6μsec pulse duration, intensity of 5E12 protons/pulse, and beam size of σ=0.1mm.

I. INTRODUCTION

Increased primary proton beam intensity and small beam spot size at the antiproton target is desirable at FNAL to maximize the phase space density of antiprotons collected. However, targeting a more intense proton beam for antiproton production exacerbates problems associated with cooling as well as with mechanical wave propagation. Previous collider runs have utilized Cu, Ta, W-Re, and Heavy Met (90% W, 6% Cu, 4% Ni) alloy disks as target materials. Of these materials, Cu exhibits the most desirable combination of thermophysical properties and is able to withstand beam intensities on the order of 2E12 protons/pulse at a repetition rate of 2 seconds and a beam size of σ=0.15mm without exhibiting evidence of target material melting or mechanical fracture.

One must consider three primary aspects when designing a target for antiproton production: selection of appropriate materials, design for thermal control (i.e., both bulk and localized beam region cooling), and optimized geometry for controlling mechanical wave propagation.

II. DESIGN CONSIDERATIONS

A. Energy Deposition Calculation

A knowledge of the energy deposition due to high energy particle beam interaction with a thick target is essential to properly design a target for antiproton production. In the present case, the energy deposition per Main Ring proton pulse has been calculated using the Monte Carlo computer code MARS10[1] which simulates the three dimensional hadron and electromagnetic cascades. The analysis assumes radial symmetry and the energy deposition per grid zone as a result of beam interaction is calculated. The result is that for a 120 GeV proton beam consisting of 5E12 protons/pulse, the total energy deposited is about 770 Joules per pulse. Assuming a repetition rate of 1.5 sec, the average power is approximately 514W.

B. Material Considerations

Material subject to a sudden deposition of beam energy experiences an instantaneous increase in pressure. The change in energy density dE and the corresponding change in hydrostatic pressure dP are related by the Mie-Grüneisen equation of state[2]:

$$dP = \Gamma \rho \, dE \qquad (1)$$

The quantity Γ is known as the Grüneisen parameter. This parameter is useful in determining the response of materials to rapid heating at constant volume and can be calculated from material thermoelastic constants.

$$\Gamma = \frac{B_t(3\alpha)}{\rho \, C_v} \qquad (2)$$

B_t is the bulk modulus, α is the linear thermal expansion coefficient, ρ is the material density, and C_v is the constant volume specific heat. The rapid heating and subsequent sudden pressure variations developed in the material due to a single beam pulse result in mechanical wave propagation. Knowledge of the quantity $\rho\Gamma$ for various materials allows one to estimate beam zone pressures as a function of energy deposition. It may be readily shown that for the same amount of energy deposition, heavy metals (e.g., tungsten) experience about twice the pressure as that experienced in copper.

The atomic structure also must be considered when selecting a suitable target material. Body-centered cubic crystals such as iron and tungsten exhibit high sensitivity to notch embrittlement and relatively low impact strength. Face centered cubic crystals, such as copper, exhibit better impact resistance. Additionally, one of the effects of radiation on structural materials is the loss of ductility. However, the face-centered cubic materials exhibit less of a tendency to become brittle when irradiated.

In addition, the target material should have high thermal conductivity to minimize temperature gradients and allow for quick heat dissipation. For these noted reasons, copper has been selected as a suitable starting point for target material selection.

C. Prototype Target Discussion - Design for Thermal and Mechanical Stress Wave Control

Practical design consideration for bulk cooling focuses on the application of a simple and reliable cooling scheme. Because of the inconvenience involved in the handling and maintenance of systems incorporating water cooling in which the water becomes tritium laden after prolonged exposure to beam environments, an air cooled target design was selected. The cooling system must dissipate the 514W generated by the beam interaction while maintaining reasonable temperature levels and gradients. Mass airflow rate and cooling channel geometry was specified to accommodate a design goal of maintaining bulk target temperatures below 175°C during service.

In addition to the bulk cooling requirements, the geometry of the target must also be designed to control the amplitude of stress waves resulting from the sudden deposition of beam energy. The basic mechanism of stress wave propagation was investigated using the finite element code ANSYS®. Mechanical analyses were conducted using the energy deposition calculations assuming a copper target subjected to a 120 GeV primary proton beam comprised of 5E12 protons/pulse with a beam size of σ=0.1mm. Initial models analyzed a simple cylindrical copper geometry of length 7cm and radius 25mm. Material in the beam region was modeled as a hydrodynamic solid using the Mie-Grüneisen equation of state to determine initial pressures. The remainder of the cylindrical target was modeled as a thermal elastic-plastic solid obeying von Mises yield criterion with kinematic hardening.

The mechanical analysis results reveal a radially outgoing compressive wave immediately after beam spill. Upon reaching the free surface, the compressive wave is reflected as an ingoing tensile wave. Due to focusing effects, the wave intensity increases with decreasing radius and a large tensile peak occurs in the region surrounding the core of maximum energy deposition. Such a tensile peak is potentially destructive. Figure 1 presents an ANSYS® plot of circumferential and radial stress vs. time, displaying such phenomena at a location 3mm from the beam centerline. The curve indicates a maximum circumferential stress of about .38 GPa (55000 psi) occuring 12 μsec after beam spill. The initial compressive and half-wavelength rarefaction peak amplitudes located near the beam immediately after beam exposure are difficult to control through geometry. However, one may control the magnitude of the reflected tensile peak

---

®ANSYS is a registered trademark of Swanson Analysis Systems, Inc.
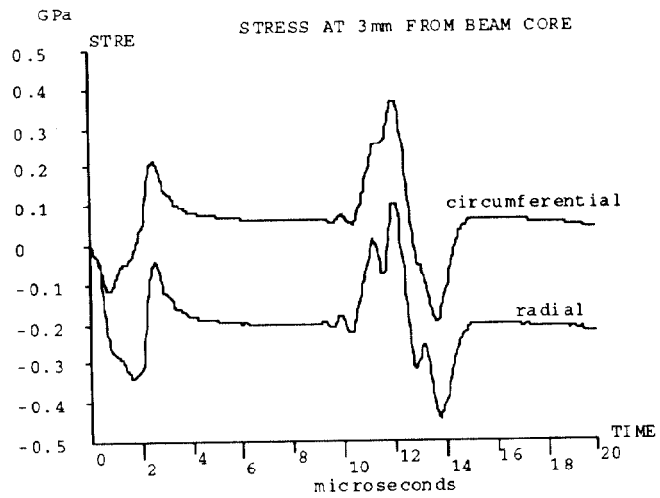
through selection of appropriate geometry.

Figure 1. ANSYS® plot of wave propagation in Cu cylinder

Figure 2 outlines the basic features of the prototype antiproton target which awaits the first stages of beamline testing. The target length is 7cm and the effective target diameter is 12.7mm. Also present are 81 cooling channels each 4.8mm in diameter. Such geometry allows sufficient area for convective heat transfer to occur. In addition, the array of holes is effective in dispersing the outgoing compressive wave which dramatically decreases the magnitude of the reflected ingoing tensile wave. Simplified one-dimensional analytical models indicate that a single layer of holes may disperse 30 to 50% (i.e., depending on spacing) of the outward travelling wave energy.
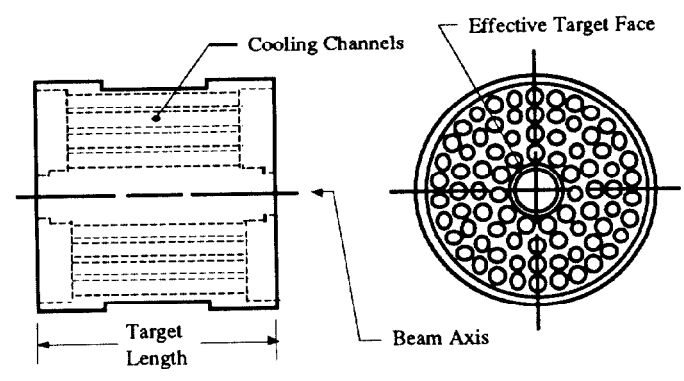

Figure 2. Prototype antiproton target core schematic.

The efficiency of the design relative to bulk cooling was verified using a simple bench test. The target core cooling channels present 616 cm² of surface area for convection cooling. Required air flow rates and heat transfer coefficients were calculated using a correlation from Seider and Tate[3] to

determine the Nusselt number for combined entry length flow (i.e., the case in which the temperature and velocity profiles develop simultaneously).

$$\overline{Nu}_D = 1.86 \left(\frac{Re_D Pr}{L/D}\right)^{1/3} \left(\frac{\mu}{\mu_s}\right)^{0.14} \tag{3}$$

Re is the dimensionless Reynolds number in the cooling channels, Pr is the Prandtl number, L is the cooling channel length, D is the cooling channel diameter, μ and μ_s is the viscosity of air evaluated at the average of the mean air temperature and the channel surface conditions, respectively. The correlation is accurate for the constant surface temperature condition (determined by experiment to be the case when using copper as the target material due to its high thermal conductivity). The heat transfer coefficient may be calculated directly using equation (3) and was estimated to be 45 W/m^2/K for an air mass flow rate of 6.577E-3 kg/sec (i.e., volumetric airflow of 12 cfm at STP). At such flow, the steady state temperature was estimated to be about 200°C. Further calculations indicated an air mass flow rate of 8.22E-3 kg/sec (i.e., volumetric airflow of 15 cfm at STP) would result in steady state temperatures of approximately 165°C.

Bulk cooling tests were conducted by machining a hole along the axis of the target core to accept a 9.5mm diameter, 7 cm length cartridge rod heater for the purpose of simulating the thermal energy deposited via beam interaction. The assembly was instrumented with thermocouples and wrapped with ceramic cloth such that convective heat transfer in the cooling channels was the only means by which input energy would be dissipated. Testing was conducted at volumetric airflow rates of 12 and 15 cfm for cartridge heater powers up to 600W. Figure 3 presents a portion of experimental data showing temperature as a function of time immediately after heater powerup through steady state at a location 8mm radially from the target centerline on the downstream face (i.e., the location of highest bulk temperature). Temperature gradients of less than 10°C were noted in all test conditions. The experimental data indicates agreement with design calculations.
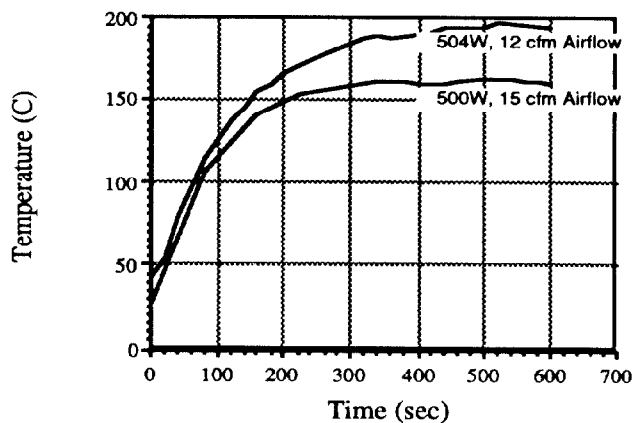

Figure 3. Thermal bench test results for 12 and 15 cfm volumetric airflow through target cooling channels

For initial beamline testing, an air delivery system consisting of a roots type blower will be incorporated. Such a system is capable of supplying continuous volumetric airflow rates of 25 cfm. An increased airflow rate over that used in the bench test coupled with natural convection occuring at the target surface and conduction heat transfer through the target mounting mechanism should result in substantially lower bulk target temperatures than those measured in the bench test.

Forthcoming beamline testing is scheduled to evaluate the design on a per pulse basis and determine if localized melting in the beam region is to occur. Should localized melting be apparent, endcaps that provide a degree of axial preload could be utilized to prevent material from spalling at the target face ends. Further testing will focus on long term fatigue effects and antiproton yield vs. the number of cumulative beam pulses.

III. REFERENCES

(1) N.V. Mokhov, Private Communication & MARS10 Manual, Fermilab FN-509, 1989.

(2) G.H. Bloom, "Grüneisen Parameter Measurements for High Explosives", in Shock Waves in Condensed Matter, New York: American Institute of Physics, 1982, pp. 588-590.

(3) F.P. Incropera and D.P. DeWitt, Fundamentals of Heat and Mass Transfer, New York: John Wiley & Sons, 1985, p. 393.